Food Chemistry 190 (2016) 460–467

Contents lists available at ScienceDirect

Food Chemistry

journal homepage: www.elsevier.com/locate/foodchem

Analytical Methods

Magnetically separable polymer (Mag-MIP) for selective analysis of biotin in food samples

Rosario Josefina Uzuriaga-Sánchez [a,c], Sabir Khan [a], Ademar Wong [a], Gino Picasso [c], Maria Isabel Pividori [b], Maria Del Pilar Taboada Sotomayor [a,*]

[a] UNESP – Univ Estadual Paulista, Institute of Chemistry, Department of Analytical Chemistry, 14801-970 Araraquara, SP, Brazil
[b] Group de Sensors i Biosensors, Departament de Química, Universitat Autònoma de Barcelona (UAB), 08193 Bellaterra, Barcelona, Spain
[c] Laboratory of Physical Chemistry Research, Faculty of Science, National University of Engineering, Tupac Amaru 210 Av., Rimac, Lima, Peru

ARTICLE INFO

Article history:
Received 17 January 2015
Received in revised form 28 May 2015
Accepted 31 May 2015
Available online 1 June 2015

Keywords:
Magnetic-MIP
Biotin
Magnetic nanoparticles
Imprinted polymers
Milk

ABSTRACT

This work presents an efficient method for the preparation of magnetic nanoparticles modified with molecularly imprinted polymers (Mag-MIP) through core–shell method for the determination of biotin in milk food samples. The functional monomer acrylic acid was selected from molecular modeling, EGDMA was used as cross-linking monomer and AIBN as radical initiator. The Mag-MIP and Mag-NIP were characterized by FTIR, magnetic hysteresis, XRD, SEM and N_2-sorption measurements. The capacity of Mag-MIP for biotin adsorption, its kinetics and selectivity were studied in detail. The adsorption data was well described by Freundlich isotherm model with adsorption equilibrium constant (K_F) of 1.46 mL g^{-1}. The selectivity experiments revealed that prepared Mag-MIP had higher selectivity toward biotin compared to other molecules with different chemical structure. The material was successfully applied for the determination of biotin in diverse milk samples using HPLC for quantification of the analyte, obtaining the mean value of 87.4% recovery.

1. Introduction

The technology of molecular imprinting is a viable synthetic approach to developed polymers with high selectivity and affinity for the target materials able to mimic natural recognition entities (Vasapollo et al., 2011). The use of molecularly imprinted polymers (MIP) has received much attention, due to its inherent advantages, such as the low cost of synthesis, high mechanical and chemical stability, as well as a highly selective recognition. MIP as a nano-spherical material, has a better performance for selective removal of trace of analytes from complex samples because of its small particle size and high specific surface area which could lead to a large amount of adsorption capacity and a fast adsorption rate (Du et al., 2014; Zhao, Zhao, & Zeng, 2014). Thus, molecularly imprinted polymers have promising applications to recognize amino acid and protein (Cai et al., 2010; Scorrano, Mergola, Del Sole, & Vasapollo, 2011), food (Song, Xu, Chen, Wei, & Xiong, 2014), pesticides (Xie, Zhou, Gao, & Li, 2010), drugs (Dai, Geissen, Zhang, Zhang, & Zhou, 2011) endocrine disrupting chemicals (Li et al., 2010), folic acid (Prasad, Tiwari, Madhuri, & Sharma, 2010) and are applied as modifiers in chemical sensors (Toro, Marestoni, & Sotomayor, 2015). In more recent applications, magnetic molecularly imprinted polymers (Mag-MIP) have been used for the recognition of antibiotics in food and environmental samples (Chen et al., 2009, 2010).

The imprinted technology is based on the formation of a complex between an analyte (template) and a selected functional monomer. In the presence of a large excess of a cross-linking agent, a three-dimensional polymer network is formed. Template is removed after polymerization from the polymer leaving to specific recognition sites which are complementary in shape, size and chemical functionality to the template molecule. Usually, intermolecular interactions (hydrogen bonds, dipole–dipole and ionic interactions) observed between the template molecule and functional groups present in the polymer matrix drive the molecular recognition phenomena.

The new core–shell synthesis is receiving widespread attention, in which molecular imprinting surface (shell) is performed over supermagnetic nanoparticles (core). The resulting material (Mag-MIP) retains its magnetic properties, and thus can still be manipulated easily by external magnetic fields, with the additional advantage of having on its surface, a selective adsorbent material (MIP) to perform recognition with high efficiency. Additionally,

* Corresponding author.
E-mail address: mpilar@iq.unesp.br (M.D.P.T. Sotomayor).

http://dx.doi.org/10.1016/j.foodchem.2015.05.129
0308-8146/

the particle size of the Mag-MIP obtained by core–shell is small enough to provide a high surface area. Moreover, the recognition sites are located on the surface of the material, facilitating the access of the analyte to the selective cavities, and its easy removal from the surface comparing to the MIP obtained by traditional synthesis methods. These advantages of Mag-MIP make these materials attractive for a wide variety of applications in biotechnology, separation techniques, and development of sensors (Chen, Huang, Zeng, Tang, & Li, 2015; Duan et al., 2015; Ma & Shi, 2015). Thus, the quantification of analytes using these materials is expected to be more sensitive and selective due to the large number of recognition sites located on the surface of MIP in each Mag-MIP particle (Chen & Li, 2013).

Biotin which also known as vitamin H is slightly water-soluble vitamin essential for the metabolism of amino acids, carbohydrates and in the syntheses of some nucleic acid. Many methods have been reported for the determination of biotin in milk and infant formulas, through immunoassay with monoclonal antibodies (Indyk et al., 2000); microbiology assays with *Lactobacillus plantarum* (Zhang et al., 2014); liquid chromatography with fluorescence detection (Gimenez, Trisconi, Kilinc, & Andrieux, 2010); HPLC with corona-charged aerosol detector (C-CAD) a new type of chromatographic detector (Márquez-Sillero, Cárdenas, & Valcárcel, 2013) or chemometric tools, using data combined from electrochemical and fluorescent measurements in a multivariate curve resolution-alternating least squares (MCR-ALS) (Gholivand, Jalalvand, Goicoechea, Gargallo, & Skov, 2015). Although all of these methods are highly sensitive, the use of biological compounds limited their robustness and increases the cost of analysis. Additionally, in the search for simpler methods, it would be appropriate to use well-established analytical methods in order to facilitate their wide applications in several laboratories. In order to achieve this, magnetic particles offer several attractive and new possibilities in food analysis, as they may be decorated with various molecules, such as MIPs, and manipulated by the application of an external magnetic field, allowing the clean-up and preconcentration of analytes in complex samples in a simple way before they are analyzed by chromatographic or spectrophotometry UV/vis techniques. To the best to our knowledge, this work describes for the first time, synthesis, optimization and application of magnetic MIPs for the rapid and selective determination of biotin in milk food samples.

2. Materials and methods

2.1. Reagents and solutions

The reagents used in this work were analytical grade. All solutions were prepared in deionized water (18 MΩ cm at 25 °C) obtained from Milli-Q Direct-0.3 (Millipore). Biotin and biocytin were acquiring from Sigma–Aldrich®. Pentylamine-Biotin and (R)-NHS-SS-biotin were acquiring from Thermo Scientific EZ-Link. The solvents with HPLC grade, dimethylformamide, acetonitrile, toluene, methanol and acetic acid were purchasing from Vetec®. Sulphuric and phosphoric acids were purchasing from Synth-Brazil®. In this work, micropipettes Eppendorf (10–100 μL and 100–1000 μL) were used. All the pH measurements were carried out in a Thermo Scientific® pH-meter (Orion 3 Star pH, Benchtop – USA).

2.2. Computer simulation

The simulation was performed by molecular mechanics using a desktop PC running Microsoft Windows XP Professional operating system. The functional monomer for the synthesis of imprinted polymer was selected from molecular modeling studies, using computer programs HyperChem® 8.0.5 and OpenEye®. Structural optimization and energy calculation were performed for the determination of the best interaction between the biotin and commonly available monomers enlisted in Table S1 of the Supplementary Data (MP1 to MP20). The results obtained showed that the MP4 (acrylic acid) presented high binding energy. Therefore, the polymers MIP and NIP (in absence of biotin) were synthesized using the acrylic acid (AA) as functional monomer.

2.3. Preparation of supermagnetic nanoparticles

Supermagnetic nanoparticles were prepared following procedure described in literature (Thach, Hai, & Chau, 2008) by mixing 0.01 mol $FeSO_4{\cdot}7H_2O$, 0.02 mol $Fe_2(SO_4)_3{\cdot}9H_2O$ and 80 mL of deionized water under mechanical stirring in nitrogen atmosphere at 80 °C. The pH of the reaction mixture was maintained between 9 and 12 with NaOH solution (2.5% w/v). The precipitate was separated from the supernatant by a neodymium magnet ($5 \times 5 \times 50$ mm) after completing the reaction and finally, was washed with de-ionized water, ethanol and then was stored in a desiccator for 3 days for the complete removal of moisture.

To evaluate the magnetic properties of Fe_3O_4, Mag-MIP and all other materials synthesized, some measurements were carried out by vibrating sample magnetometry (VSM) in a Lakeshore VSM 7300 series instrument.

2.4. Preparation of Mag-MIP by core–shell

The prepared magnetic nanoparticles (Fe_3O_4) were treated by the sol–gel process with tetraethyl orthosilicate (TEOS) in order to introduce hydroxyl groups on the surface of the magnetic particles allowing them their subsequent silanization (Kong, Gao, He, Chen, & Zhang, 2012). With this aim, 300 mg of magnetic nanoparticles were dispersed in 40 mL of ethanol and 4 mL of ultrapure water by ultra-sonication for 15 min and then followed by the addition of 5 mL of 28% (v/v) NH_4OH and 2 mL of TEOS. The mixture was stirred for 12 h at room temperature (25 °C). The product was collected by magnetic separation and washed with ultrapure water and then dried under the vacuum. In the next step, $Fe_3O_4@SiO_2$ were modified by 3-metacriloxipropiltrimetoxissilano (MPS) taking 250 mg of this material and dispersed in 50 mL of anhydrous toluene containing 5 mL of MPS and the mixture was allowed to react for 12 h under dry nitrogen. The mixture was separated by an external magnet, washing by water and drying in vacuum, obtaining the silanized material $Fe_3O_4@SiO_2$–MPS. Then, Mag-MIP (Fe_3O_4@MIP) was prepared by polymerization of 0.2 mmol of biotin and 0.8 mmol of acrylic acid (AA) in 30 mL of ethanol (porogenic solvent). The mixture was shaken in water bath at 25 °C for 12 h, then 200 mg of $Fe_3O_4@SiO_2$–MPS were added into the system and was shaking for another 3 h. Furthermore, 4.0 mmol of ethylene glycol dimethacrylate (EGDMA) and 0.05 mmol of azoisobutyronitrile (AIBN) were added into the system and the mixture was sonicated at environment temperature for 5 min. Nitrogen gas was purged for 5 min to remove oxygen and the system was left at 60 °C under nitrogen gas protection for 24 h, obtaining the Fe_3O_4@MIP material with biotin. Afterwards, template molecule was removed after polymerization by soxhlet extraction using a ratio of methanol: acetic acid (9:1, v/v) as eluent, which was replaced every 12 h. The template has been considered completely removed when no analyte was detected in eluent by HPLC at 220 nm. The obtained product, Mag-MIP (Fe_3O_4@MIP without biotin) was dried at 40 °C under vacuum. The schematic diagram of the preparation of Mag-MIP is shown in Scheme 1.

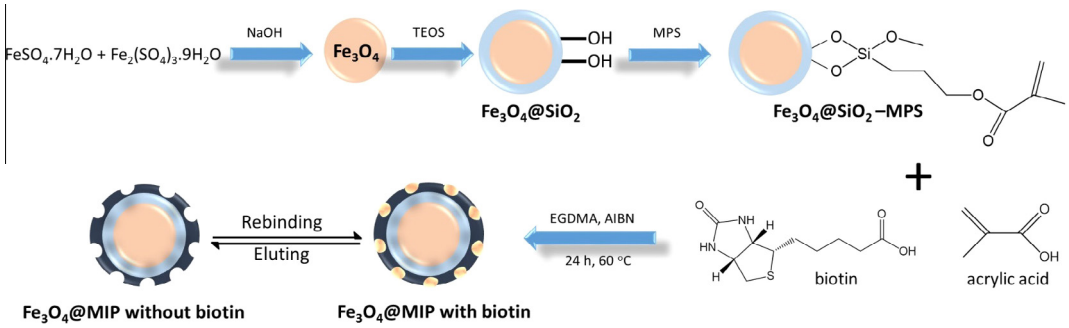

Scheme 1. Illustrative representation for the synthesis of Mag-MIP for detection of biotin proposed in this work.

The magnetic non-molecular imprinted polymer (Mag-NIP) was also prepared in order to compare its behavior with the magnetic molecular imprinted polymer (Mag-MIP) (Tarley, Sotomayor, & Kubota, 2005). For this, the procedures were the same until the polymerization with acrylic acid, which was carried out in absence of the biotin, unlike of the Mag-MIP.

2.5. HPLC analysis

The chromatographic analyses were performed using a Shimadzu Model 20A liquid chromatograph, coupled to an SPD-20A UV–Vis detector, an SIL-20A autosampler and a DGU-20A5 degasser. The chromatography system was controlled by a microcomputer and the C18 column (5 μm, 250 mm × 4.6 mm) was used in the analysis. The measurements were carried out at 25 °C in isocratic mode with mobile phase composed of a mixture of $Na_2H_2PO_4$ 25 mmol L^{-1}: methanol in the volume ratio of 80:20, flow rate of 1.0 mL min^{-1}, sample injection volume of 20 μL and wavelength of 210 nm.

Biotin stock solution was prepared in a mixture of hot water: methanol (30:70, v/v) and standard solutions between 5 and 200 mg L^{-1} were prepared from the dilution of the stock solution in methanol.

2.6. Binding and selective adsorption experiments

The binding experiments were carried out by mixing 10 mg of Mag-MIP or Mag-NIP with 10.0 mL of biotin standard solutions in concentrations from 5 to 200 mg L^{-1}. The mixture was shaken in a rotary shaker for 120 min. The magnetic polymer suspensions were separated by external neodymium magnetic bar and the remaining solution was filtered through a 0.45 μm membrane just before the HPLC analysis (procedure A).

In addition, Mag-MIP with biotin was placed in 5.0 mL of methanol, shaken for 3 h to extract the retained biotin and quantified by the HPLC method previously described in Section 2.5.

The binding capacity was calculated by the following equation:

$$Q_e = \frac{(C_0 - C_e)V}{m} \quad (1)$$

where Q_e (mg g^{-1}) is the experimental equilibrium adsorption capacity, C_0 (mg L^{-1}) is the initial concentration of analyte, C_e (mg L^{-1}) is the equilibrium concentration of analyte, V (mL) is the volume of solution and m (g) is the weight of Mag-MIP or Mag-NIP.

For the selectivity, different competitive adsorption experiments were carried out using different compounds, with analogous or different structure of the biotin. In the first case, biocytin, pentylamine-biotin, NHS-SS-biotin and in the second case, 1-chloro-2,4-dinitrobenzene. Thus, distribution coefficient (K_d, mL g^{-1}), selectivity (α), imprinting factor (I) and the relative selectivity coefficient (β) were calculated by the following Eqs. (2)–(5) (Clausen, Visentainer, & Tarley, 2014, Tarley et al., 2005).

$$K_d = \frac{Q_e}{C_e} \quad (2)$$

$$\alpha = \frac{K_{d(\text{biotin})}}{K_{d(\text{analyte})}} \quad (3)$$

$$I = \frac{K_{d(\text{Mag-MIP})}}{K_{d(\text{Mag-NIP})}} \quad (4)$$

$$\beta = \frac{\alpha_{\text{Mag-MIPs}}}{\alpha_{\text{Mag-NIPs}}} \quad (5)$$

where $\alpha_{\text{Mag-MIPs}}$ and $\alpha_{\text{Mag-NIPs}}$ are selectivity coefficient of magnetic MIP and NIP, respectively.

2.7. Selectivity experiments

The experiments were performed under the same optimized experimental conditions in presence of other compounds besides biotin in order to study selectivity of Mag-MIP to analyte. The applied specific conditions were: 10 mg of Mag-MIP, mixed with 2.5 mL of biotin and 2.5 mL of the other compound, both of them at 10 mg L^{-1}. In this study biocytin, pentylamine-biotin, NHS-SS-biotin and 1-chloro-2,4-dinitrobenzene (CDNB) were evaluated. The mixture was shaken in a rotary shaker for 120 min. The magnetic polymer suspensions were separated following procedure A.

2.8. Preparation of samples

The prepared Mag-MIP was evaluated for the analyses of biotin in milk samples. Raw milk samples were obtaining directly from the dairy farm; meanwhile skimmed milk and milk powder were collected from the supermarket at the region of Araraquara – SP, Brazil. The milk was purposely enriched with biotin at a concentration of 5 mg g^{-1}. With this aim, 0.2 g of liquid or powder milk, was mixed with 1 mg of biotin in 30 mL of sulfuric acid (1 mol L^{-1}) under stirring for 30 min at 120 °C. The mixture was allowed to cool to room temperature and the pH was adjusted between 6 and 7 using a solution of NaOH (2 mol L^{-1}). Finally, the mixture was filtered through quantitative filter paper and completed the volume to 100 mL with methanol.

Then, 10.0 mL (equivalent to 0.1 mg of biotin) of each enriched milk sample was mixed with 10 mg of Mag-MIP in different glass vials and shaken in a rotary shaker for 120 min. The magnetic polymer suspensions were separated following procedure A. Each procedure was performed in triplicate.

2.9. Statistical analysis and method validation

All measurements were performed at least in triplicate, and treated statistically using average arithmetic mean and it was calculated their corresponding standard deviation.

The method was validated by the recovery obtained from the amounts found and added. The corresponding percentage was calculated by the following relationship (Eq. (6)):

$$\% \text{ recovery} = \frac{\text{Found}}{\text{Added}} \times 100 \quad (6)$$

3. Results and discussion

3.1. Characterization of the Mag-MIP

3.1.1. Scanning electronic microscopy (SEM)

The SEM images obtained through core–shell synthesis are depicted in Fig. 1. In the Fig. 1A, it can be observed that the magnetic nanoparticles (Fe_3O_4) were obtained with an approximate diameter of 15 nm. From Fig. 1B (Fe_3O_4@SiO_2) is possible to observe that the magnetic particles are coated completely with the TEOS and in Fig. 1C with MPS (Fe_3O_4@SiO_2–MPS), they apparently are retaining its spherical shape and having in each case, an average diameter of 200 and 565 nm, respectively. The spherical-like particles of Mag-MIP are observed in Fig. 1D, with the formation of agglomerations with an average diameter of 990 nm.

3.1.2. Fourier transforms Infrared spectroscopy (FTIR)

The FT-IR spectra of Fe_3O_4, Fe_3O_4@SiO_2–TEOS, Fe_3O_4@SiO_2–MPS, Fe_3O_4@MIP and Fe_3O_4@NIP are shown in Figure S1(a) in the Supplementary Data. In the spectrum of Fe_3O_4 the peak at 574 cm^{-1} was assigned to the stretching of Fe–O bond. In the spectrum of Fe_3O_4@SiO_2–TEOS three characteristic peaks are observed: at 1093 cm^{-1}, due to Si–O–Si, at 1628 cm^{-1} corresponding to OH group and at 3405 cm^{-1} assigned to the formation of silica coated on the surface of Fe_3O_4. It is also observed from the Fe_3O_4@SiO_2–MPS spectrum the C═O group at 1700 cm^{-1} indicates that the MPS silanization was successfully performed on the surface of Fe_3O_4@SiO_2–TEOS. The peak at 2987 cm^{-1} corresponding to the C—H bond in the methyl group of the acrylic acid indicate that the polymer was successfully formed on the surface of Fe_3O_4@SiO_2–MPS. Moreover, the spectra of Fe_3O_4@MIP and Fe_3O_4@NIP had the same characteristic peaks, suggesting the complete removal of the template (biotin). These results suggest that the coatings on the surface of the Mag-MIP (Fe_3O_4@MIP) and Mag-NIP (Fe_3O_4@NIP) were performed satisfactorily. It can also observe from the Fig. S1(b), the absence of peak at 1670–1640 cm^{-1} from the stretching vinyl groups of monomers in all the synthesized polymers, probably attributable to the breakage of C═C bonds in the polymerization process yielding single bonds (Men et al., 2012).

3.1.3. Surface area (BET analysis)

The surface area is one of the most important physical parameter for characterizing novel porous materials. The BET analysis is the standard method for determining surface areas from nitrogen adsorption isotherms and was originally derived for multilayer gas adsorption onto flat surfaces (Brunauer, Emmett, & Teller, 1938). In Fig. S2 it is possible to observe significant differences in the surface area for the Mag-MIP in relation of the other materials. The Mag-MIP presents the highest surface area (120 $m^2\ g^{-1}$) suggesting the formation of cavities in the imprinted polymer. The results show that the surface area of Mag-MIP is 15.6 times higher than the corresponding to Mag-NIP. The increasing number of pores introduced in the imprinted polymer is due to the presence of Mag-MIP selective cavities (Marestoni et al., 2014). Similarly, the surface area of MIP (without magnetic particles) is 12.9 times higher than the corresponding to NIP.

The adsorption profile for all materials correspond to a classic asymmetrical hysteresis of type H2 (Golker, Karlsson, Wiklander, Rosengren, & Nicholls, 2015) which is typical for pores with narrow necks and wide bodies (Sing et al., 1985), often referred to as ink-bottle pores, and this is coherent with the biotin structure and the results obtained in the selectivity studies, from which, it was inferred that the imidazolyl ring of biotin is concentrated into the cavity of the MIP. On the other hand, the H2-like isotherm is typical of acrylic polymers (Golker et al., 2015). Similar sorption profiles showed NIP and Mag-NIP materials which have a less pronounced asymmetric profile that the corresponding MIPs, as a consequence of the absence of template forming the selective cavities. The isotherms with H2-hysteresis profile is explained as a consequence of the evaporation of the condensed liquid controlled not only by the diameter of the pore necks, but also by the interconnectivity of the pore network as well as the state of evaporation of the neighboring pores (Grosman & Ortega, 2008; Lowell, Shields, Thomas, & Thommes, 2006). Thus, the asymmetrical hysteresis loops with evaporation branches are steeper than the corresponding condensation branches located at high capillary condensation pressures (>0.8P_0). This behavior is characteristic for mesoporous materials (average diameter of pore between 2 up to 50 nm), which is consistent with data showed in Table S2 and with the corresponding to acrylate-MIPs (Marestoni et al., 2014).

3.1.4. Measurements of vibrating sample magnetometry (VSM)

Magnetization curves are shown in the Fig. 2, in which no magnetic hysteresis was observed in all cases. The absence of hysteresis (graphics are perfectly symmetrical) and coercivity (the middle point of the graphics is zero) revealed that all studied materials (from magnetite to Mag-MIP) depicted supermagnetic behavior (Zhao et al., 2013). At room temperature, the saturation (magnetic) values obtained for Fe_3O_4, Fe_3O_4@SiO_2–TEOS, Fe_3O_4@SiO_2–MPS and Fe_3O_4@MIP, were 58.5, 27.8, 5.35 and 0.55 emu g^{-1} respectively. The saturation value of the Fe_3O_4 nanoparticles obtained in this work is higher than synthesized by Zhao's group (Zhao et al., 2013). The saturation (magnetic) value of Fe_3O_4@MIP was decreased by over 100-fold compared with the pure Fe_3O_4, which is perfectly expected, since in each step of the modification, the super-paramagnetic magnetite was surrounded by layers of non-magnetic materials, allowing the magnetism of the material decrease successively. This can be explained due to the increase in the average diameter of the particles. However, the obtained material preserved a strong magnetic behavior as is showed in Fig. S3, in which an efficient separation of the Mag-MIP is observed at room temperature under an external magnetic field (neodymium magnet).

3.1.5. X-ray diffraction (XRD)

In order to elucidate the crystal structure of the material, the technique of X-ray diffraction (XRD) was applied for samples Fe_3O_4, Fe_3O_4@SiO_2–TEOS and Fe_3O_4@MIP. In all cases, the presence of six characteristic peaks located at 2θ of 27.20°, 35.58°, 43.14°, 53.48°, 57.08° and 62.66° corresponding to Fe_3O_4 in the materials was observed. The difractograms of samples showed the planes (220), (311), (400), (422), (511) and (440) corresponding to a pure cubic spinel crystal structure of Fe_3O_4 (Pan et al., 2014).

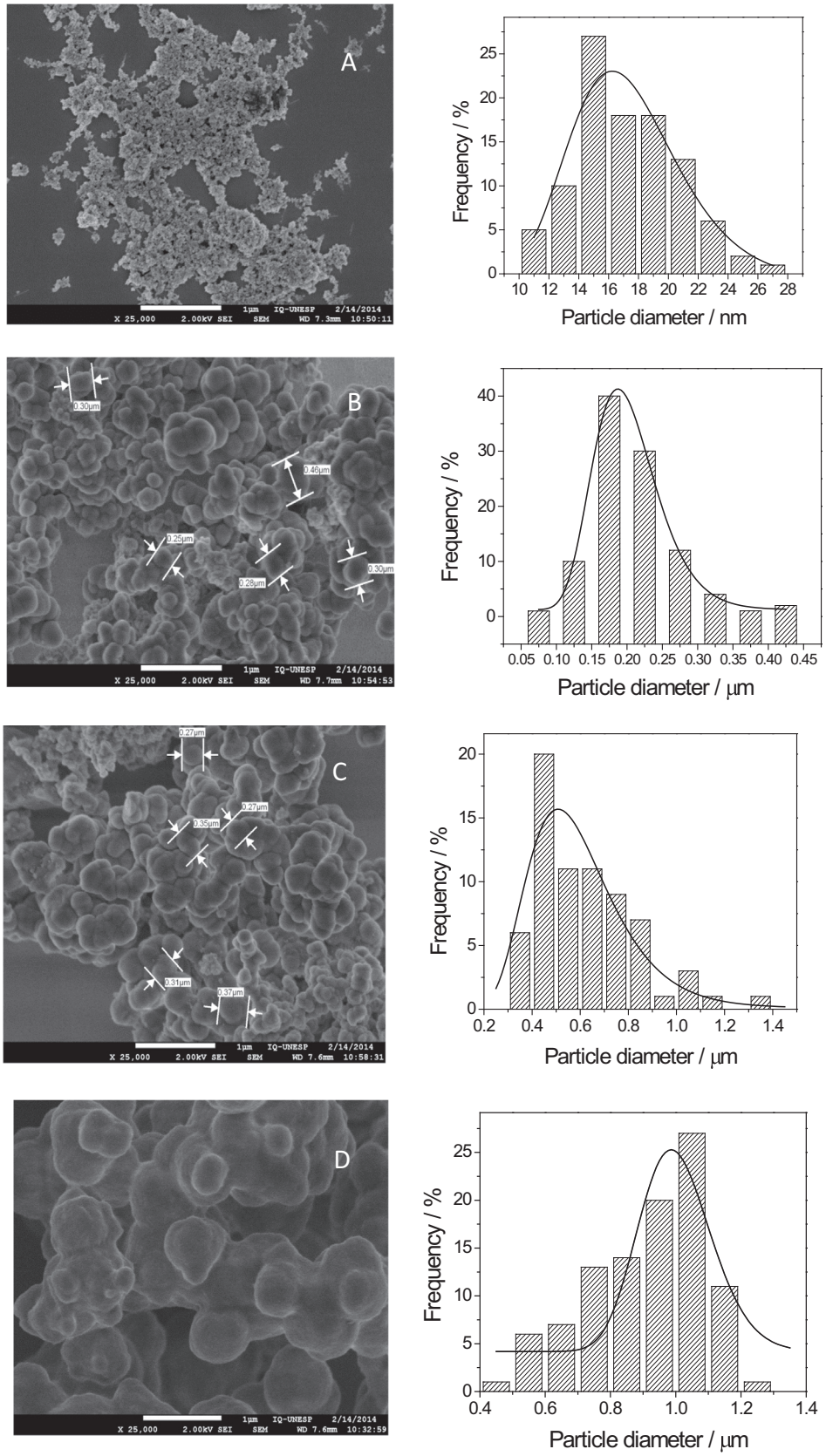

Fig. 1. SEM micrographs and graphs with the corresponding determination of average diameter of particles. (A) Fe_3O_4; (B) Fe_3O_4@SiO_2; (C) Fe_3O_4@SiO_2–MPS; (D) Fe_3O_4@MIP.

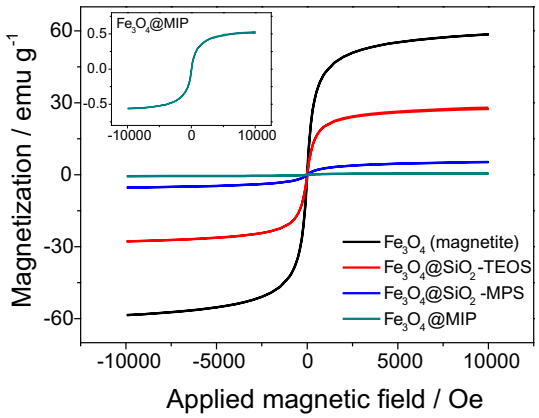

Fig. 2. The magnetization curves of Fe_3O_4 (with amplification in the inset), Fe_3O_4@SiO_2–TEOS, Fe_3O_4@SiO_2–MPS and Fe_3O_4@MIP.

3.2. Optimizing the Mag-MIP efficiency

3.2.1. Effect of dosage of Mag-MIP on the sorption of biotin

The dosage amount of Mag-MIPs and its influence in the adsorption capacity of biotin (Q value) was optimized as is presented in Fig. S4. As is observed, the Q value rapidly increased with increasing the amount of Mag-MIP (dose in mg) up to 10 mg of the polymer. Further quantities of polymer made the adsorption capacity value to decrease, remaining relatively constant after 50 mg of magnetic polymer. Consequently, the quantity of 10 mg was chosen for subsequent experiments. All experiments were carried out in triplicate.

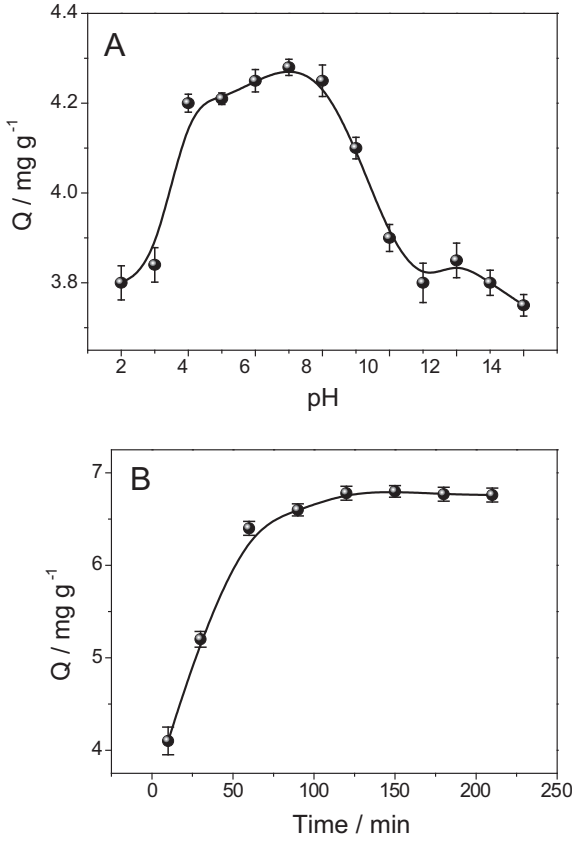

Fig. 3. (A) pH and (B) time effects on the adsorption of Mag-MIPs synthesized. Measurements carried out in triplicate.

3.2.2. Effect of pH on the sorption of biotin

Fig. 3A shows the adsorption capacity of biotin onto Mag-MIP at various pH values. In order to make this study, a quantity of 10 mg of Mag-MIP was added to 13 vials and mixed with 10.0 mL of biotin standard solution (10 mg L^{-1}). The pH of each solution was adjusted between 2 and 14. The mixtures were stirred for 2 h, in order to reach the equilibrium with the maximum value of adsorption of analyte by the polymer. The results showed that at pH range from 4 to 9 correspond to the higher values of adsorption of biotin with a maximum at pH = 7. Therefore, neutral pH was selected for further experiments. Low adsorption capacity observed for pH < 3 is probably due to both the biotin and the imprinted polymer, which are fully protonated. In fact, once the analyte possesses a pK_a of 4.5 (Said, 2009), at pH ranging from 1 to 3, the carboxylic group remains completely protonated in crosslinked copolymers of acrylic acid (Gaballa, Geever, Killion, & Higginbotham, 2013). This would explain an electrostatic repulsion of the biotin in the selective cavity of MIP. On the other hand, in the pH interval between 4 and 9, the biotin is totally negatively charged making easier its interaction with carboxylic acids of the protonated poly(acrylic acid) in the MIP. Finally, at pH values higher than 10, the COOH group of crosslinked polymers of acrylic acid is totally deprotonated (COO–) and negatively charged (Gaballa et al., 2013) producing electrostatic repulsion of biotin also negatively charged and, as a consequence, decreasing the adsorptive capacity of the analyte in the MIP.

3.3. Adsorption kinetics of biotin

It is important to study the adsorption kinetics because it provides valuable information of both the adsorption process and the rate-controlling mechanism. Fig. 3B shows the time dependence of adsorption capacity of biotin onto Mag-MIP, considering the values of initial concentration, temperature and pH of the system equal to 10 mg L^{-1}, 25 °C and 7, respectively. The Fig. 3B reveals that the uptake rates of biotin were initially fast, reaching a maximum at 120 min and then became almost constant. Therefore, a time adsorption of 120 min was selected for further analysis. The first-order and second-order models were applied to evaluate the kinetics of sorption process (Ho, 2006). The first-order and second-order equations are given by Eqs. (6) and (7), respectively.

$$\ln(Q_e - Q_t) = \ln Q_e - K_1 t \tag{7}$$

$$\frac{1}{Q_t} = \frac{1}{k_2 Q_e^2} + \frac{1}{Q_e} t \tag{8}$$

where Q_e and Q_t are the amounts of biotin adsorbed (mg g^{-1}) on the sorbent at equilibrium and at time t (min), respectively. K_1 (min^{-1}) and K_2 (mg g^{-1} min^{-1}) are the first and second-order rate constants, respectively, calculated from the linear plots of ln ($Q_e - Q_t$) versus t and t/Q_t versus t. Corresponding equations, rate constants and regression coefficient (R) for Mag-MIP are summarized in the Table S3 in Supplementary Data of Section S5. It is observed that R for the second-order kinetic model (0.9990) was found to be obviously higher than the corresponding to the first-order equation. Consequently, the second-order model describes much better the kinetic adsorption data of biotin onto Mag-MIP. Other kinetic studies involving biotin adsorption onto Mag-MIP are presented in the Supplementary Data, in Section S5.

3.4. Selectivity of Mag-MIP

The results of the selectivity studies of Mag-MIP to biotin are shown in Table 1 and the corresponding chromatograms are

Table 1
Distribution coefficients (K_d), selectivity (α), imprinting factor (I) and relative selectivity coefficients (β) calculated from studies of selectivity performed with Mag-MIP.

Analytes	Mag-MIP		Mag-NIP		$I_{MIP/NIP}$	$\beta_{MIP/NIP}$
	K_d (mL g^{-1})	α	K_d (mL g^{-1})	α		
Biotin	1152.8	2.40	684.6	1.2	1.68	1.90
Biocytin	480.38		541.07		0.88	
Biotin	323.5	2.54	315	2.45	1.026	1.04
Biotin-pent	127		128.2		0.99	
Biotin	280.5	1.52	264	1.076	1.06	1.41
NHS-SS-biotin	185		245.3		0.75	
Biotin	241	63.42	253	12.65	0.95	5.0
CDBN	3.8		20		0.19	

Table 2
Recovery of biotin in different milk samples using Mag-MIP. The amount of biotin added was 5.0 mg g^{-1}. Standard deviation for triplicates.

Sample	Biotin found	Recovery/%
Milk powder	3.9 ± 0.7	77 ± 14
Raw cow's milk	4.2 ± 0.2	83 ± 4
Skimmed milk	5.1 ± 0.1	102 ± 2

showed in S6, S8–S11. The results indicated that Mag-MIP showed maximum adsorption capacity to biotin, due to the probable presence of nanocavities with selective size and shape as well as to an effect of specific interactions. This was more evident for CDNB, which has a different chemical structure of biotin. However, for the analogous compounds, the β values (relative selectivity) were only slightly higher than unit. This means that Mag-MIP may also be used in the case of other biotinylated molecules with practically the same selectivity than with the simple biotin, since such as described in Section 3.1.3, the moiety of biotin and analogues compounds are able to fit imidazolyl group of the molecule inside the selective cavity of the MIP. This may be useful in the development of biomimetic immunoassays. Additionally, since all molecules tested have in their structure biotin, it could infer that the cavity formed in the Mag-MIP is complementary to this molecule, revealing the success in the synthesis of this new selective material.

3.5. Validation and application of the proposed method

The most common application of MIPs is as adsorbent materials. For this reason, the Mag-MIP was evaluated on extraction, clean up and pre-concentration of samples of raw, skimmed and powder of milk. The experiments were performed such as described in Section 2.8 and the biotin quantification was carried out from procedure described in Section 2.5. Under these conditions, the dynamic range for biotin quantification was from 5.0 to 100 mg L^{-1}, with a detection limit of 0.96 mg L^{-1} (Figs. S6 and S7). The main advantage of the application of selective magnetic particles was the use of simple neodymium magnet for separation purposes, avoiding loss of analyte and possible failures in its quantification.

As is shown in Table 2, the % recoveries obtained in this work were quite well high ranging from 77.4% to 101.8%, attesting the accuracy and applicability of the proposed material (Table 2).

4. Conclusion

This work introduced a new concept to prepare Mag-MIP for analyzing complex target molecule like biotin in the real milk samples. The prepared Mag-MIP exhibited strong magnetic responsiveness, good reproducibility, high adsorption capacity, good selectivity and quick kinetics. The obtained imprinted Fe_3O_4@MIP sphere nanostructures show the excellent magnetic properties of Fe_3O_4 core, allowing them the direct capture and easy separation of targets in complex samples by an external magnetic field. The Mag-MIP shows high recoveries at practical concentration range and opens a new window for analyzing compounds in high complex food samples, among them for instance, the determination of antibiotics in milk and pesticides in vegetables, which is now developed in our research group.

Acknowledgements

The authors are thankful to National Council for Scientific and Technological Development (CNPq) Brazil for the financial support for this research project under the science without borders program (Processes 4004759/2012-4, 303979/2012-7 and 151525/2013-7).

Appendix A. Supplementary data

Supplementary data associated with this article can be found, in the online version, at http://dx.doi.org/10.1016/j.foodchem.2015.05.129.

References

Brunauer, S., Emmett, P. H., & Teller, E. (1938). Adsorption of gases in multimolecular layers. *Journal of the America Chemical Society, 60*, 309–319.
Cai, D., Ren, L., Zhao, H., Xu, C., Zhang, L., Yu, Y., et al. (2010). A molecular-imprint nanosensor for ultrasensitive detection of proteins. *Nature Nanotechnology, 5*(8), 597–601.
Chen, J., Huang, H., Zeng, Y., Tang, H., & Li, L. (2015). A novel composite of molecularly imprinted polymer-coated PdNPs for electrochemical sensing norepinephrine. *Biosensors and Bioelectronics, 65*, 366–374.
Chen, L., & Li, B. (2013). Magnetic molecularly imprinted polymer extraction of chloramphenicol from honey. *Food Chemistry, 141*(1), 23–28.
Chen, L., Zhang, X., Sun, L., Xu, Y., Zeng, Q., Wang, H., et al. (2009). Fast and selective extraction of sulfonamides from honey based on magnetic molecularly imprinted polymer. *Journal of Agricultural and Food Chemistry, 57*(21), 10073–10080.
Chen, L., Zhang, X., Xu, Y., Du, X., Sun, X., Sun, L., et al. (2010). Determination of fluoroquinolone antibiotics in environmental water samples based on magnetic molecularly imprinted polymer extraction followed by liquid chromatography-tandem mass spectrometry. *Analytica Chimica Acta, 662*(1), 31–38.
Clausen, D. N., Visentainer, J. V., & Tarley, C. R. T. (2014). Development of molecularly imprinted poly(methacrylic acid)/silica for clean-up and selective extraction of cholesterol in milk prior to analysis by HPLC-UV. *The Analyst, 139*(19), 5021–5027.
Dai, C.-M., Geissen, S.-U., Zhang, Y.-L., Zhang, Y.-J., & Zhou, X.-F. (2011). Selective removal of diclofenac from contaminated water using molecularly imprinted polymer microspheres. *Environmental Pollution (Barking, Essex: 1987), 159*(6), 1660–1666.
Du, X., Lin, S., Gan, N., Chen, X., Cao, Y., Li, T., et al. (2014). Multi-walled carbon nanotube modified dummy-template magnetic molecularly imprinted microspheres as solid-phase extraction material for the determination of polychlorinated biphenyls in fish. *Journal of Separation Science, 37*(13), 1591–1600.
Duan, H., Li, L., Wang, X., Wang, Y., Li, J., & Luo, C. (2015). A sensitive and selective chemiluminescence sensor for the determination of dopamine based on

silanized magnetic graphene oxide-molecularly imprinted polymer. *Spectrochimica Acta Part A: Molecular and Biomolecular Spectroscopy, 139*, 374–379.

Gaballa, H. A., Geever, L. M., Killion, J. A., & Higginbotham, C. L. (2013). Synthesis and characterization of physically crosslinked N-vinylcaprolactam, acrylic acid, methacrylic acid, and N,N-dimethylacrylamide hydrogels. *Journal of Polymer Science Part B-Polymer Physics, 51*(21), 1555–1564.

Gholivand, M.-B., Jalalvand, A. R., Goicoechea, H. C., Gargallo, R., & Skov, T. (2015). Chemometrics: An important tool for monitoring interactions of vitamin B7 with bovine serum albumin with the aim of developing an efficient biosensing system for the analysis of protein. *Talanta, 132*, 354–365.

Gimenez, E. C., Trisconi, M. J., Kilinc, T., & Andrieux, P. (2010). Optimization and validation of an LC-FLD method for biotin in infant formula, infant cereals, cocoa-malt beverages, and clinical nutrition products. *Journal of AOAC International, 93*(5), 1494–1502.

Golker, K., Karlsson, B. C. G., Wiklander, J. G., Rosengren, A. M., & Nicholls, I. A. (2015). Hydrogen bond diversity in the pre-polymerization stage contributes to morphology and MIP-template recognition – MAA versus MMA. *European Polymer Journal, 66*, 558–568.

Grosman, A., & Ortega, C. (2008). Capillary condensation in porous materials hysteresis and interaction mechanism without pore blocking/percolation process. *Langmuir, 24*(8), 3977–3986.

Ho, Y.-S. (2006). Review of second-order models for adsorption systems. *Journal of Hazardous Materials, 136*(3), 681–689.

Indyk, H. E., Evans, E. A., Caselunghe, M. C. B., Persson, B. S., Finglas, P. M., Woollard, D. C., et al. (2000). Determination of biotin and folate in infant formula and milk by optical biosensor-based immunoassay. *Journal of AOAC International, 83*(5), 1141–1148.

Kong, X., Gao, R., He, X., Chen, L., & Zhang, Y. (2012). Synthesis and characterization of the core-shell magnetic molecularly imprinted polymers (Fe_3O_4@MIPs) adsorbents for effective extraction and determination of sulfonamides in the poultry feed. *Journal of Chromatography A, 1245*, 8–16.

Li, Y., Li, X., Chu, J., Dong, C., Qi, J., & Yuan, Y. (2010). Synthesis of core-shell magnetic molecular imprinted polymer by the surface RAFT polymerization for the fast and selective removal of endocrine disrupting chemicals from aqueous solutions. *Environmental Pollution (Barking, Essex : 1987), 158*(6), 2317–2323.

Lowell, S., Shields, J. E., Thomas, M. A., & Thommes, M. (2006). *Characterization of porous solids and powders: Surface area, pore size and density*. Netherlands: Springer. 2006.

Ma, R.-T., & Shi, Y.-P. (2015). Magnetic molecularly imprinted polymer for the selective extraction of quercetagetin from Calendula officinalis extract. *Talanta, 34*, 650–656.

Marestoni, L. D., Wong, A., Feliciano, G. T., Marchi, M. R. R., Tarley, C. R. T., & Sotomayor, M. D. P. T. (2014). Optimization and application of imprinted poly(AA-EGDMA) for solid phase extraction of ciprofloxacin in artificial urine. *Curr Drug Therapy, 9*(4), 270–276.

Márquez-Sillero, I., Cárdenas, S., & Valcárcel, M. (2013). Determination of water-soluble vitamins in infant milk and dietary supplement using a liquid chromatography on-line coupled to a corona-charged aerosol detector. *Journal of Chromatography A, 1313*, 253–258.

Men, H.-F., Liu, H.-Q., Zhang, Z.-L., Huang, J., Zhang, J., Zhai, Y.-Y., et al. (2012). Synthesis, properties and application research of atrazine Fe_3O_4@SiO_2 magnetic molecularly imprinted polymer. *Environmental Science and Pollution Research International, 19*(6), 2271–2280.

Pan, S. D., Shen, H. Y., Zhou, L. X., Chen, X. H., Zhao, Y. G., Cai, M. Q., et al. (2014). Controlled synthesis of pentachlorophenol imprinted polymers on the surface of magnetic graphene oxide for highly selective adsorption. *Journal of Materials Chemistry A, 2*, 15345–15356.

Prasad, B. B., Tiwari, M. P., Madhuri, R., & Sharma, P. S. (2010). Development of a highly sensitive and selective hyphenated technique (molecularly imprinted micro-solid phase extraction fiber-molecularly imprinted polymer fiber sensor) for ultratrace analysis of folic acid. *Analytica Chimica Acta, 662*(1), 14–22.

Said, H. M. (2009). Cell and molecular aspects of human intestinal biotin absorption. *The Journal of Nutrition, Symposium: Advances in Understanding of the Biological Role of Biotin at the Clinical, Biochemical and Molecular Level*, 158–162.

Scorrano, S., Mergola, L., Del Sole, R., & Vasapollo, G. (2011). Synthesis of molecularly imprinted polymers for amino acid derivates by using different functional monomers. *International Journal of Molecular Sciences, 12*(3), 1735–1743.

Sing, K. S. W., Everett, D. H., Haul, R. A. W., Moscou, L., Pierotti, R. A., Rouquerol, J., et al. (1985). Reporting physisorption data for gas solid systems with special reference to the determination of surface-area and porosity. *Pure Applied Chemistry, 57*(4), 603–619.

Song, X., Xu, S., Chen, L., Wei, Y., & Xiong, H. (2014). Recent advances in molecularly imprinted polymers in food analysis. *Journal of Applied Polymer Science, 131*(16), 40766.

Tarley, C. R. T., Sotomayor, M. D. P. T., & Kubota, L. T. (2005). Polímeros biomiméticos em química analítica. Parte 1: preparo e aplicações de MIP (''Molecularly Imprinted Polymers'') em técnicas de extração e separação. *Química Nova, 28*(6), 1076–1086.

Thach, C. V., Hai, N. H., & Chau, N. (2008). Size controlled magnetite nanoparticles and their drug loading ability. *Journal of the Korean Physical Society, 52*(5), 1332.

Toro, M. J. U., Marestoni, L. D., & Sotomayor, M. D. P. (2015). A new biomimetic sensor based on molecularly imprinted polymers for highly sensitive and selective determination of hexazinone herbicide. *Sensors and Actuators B, 208*, 299–306.

Vasapollo, G., Sole, R. . Del., Mergola, L., Lazzoi, M. R., Scardino, A., Scorrano, S., et al. (2011). Molecularly imprinted polymers: Present and future prospective. *International Journal of Molecular Sciences, 12*(9), 5908–5945.

Xie, C., Zhou, H., Gao, S., & Li, H. (2010). Molecular imprinting method for on-line enrichment and chemiluminescent detection of the organophosphate pesticide triazophos. *Microchimica Acta, 171*(3–4), 355–362.

Zhang, H., Lan, F., Shi, Y., Wan, Z., Yue, Z., Fan, F., et al. (2014). A ''three-in-one'' sample preparation method for simultaneous determination of B-group water-soluble vitamins in infant formula using VitaFast® kits. *Food Chemistry, 153*, 371–377.

Zhao, Y.-G., Chen, X.-H., Pan, S.-D., Zhu, H., Shen, H.-Y., & Jin, M.-C. (2013). Self-assembly of a surface bisphenol A-imprinted core–shell nanoring amino-functionalized superparamagnetic polymer. *Journal of Materials Chemistry A, 1*(38), 11648.

Zhao, L., Zhao, F., & Zeng, B. (2014). Synthesis of water-compatible surface-imprinted polymer via click chemistry and RAFT precipitation polymerization for highly selective and sensitive electrochemical assay of fenitrothion. *Biosensors & Bioelectronics, 62*, 19–24.